



Intestinal stem cell-derived extracellular vesicles ameliorate necrotizing enterocolitis injury

Le Zhang^{a,f,1}, Jiahong Li^{b,1}, Qiwen Wan^{c,1}, Chaozhi Bu^d, Weilai Jin^{a,**},
Fuqiang Yuan^{a,***}, Wenhao Zhou^{e,f,*}

^a Department of Neonatology, Affiliated Children's Hospital of Jiangnan University, Wuxi Children's Hospital, 214023, Wuxi, Jiangsu, China

^b Department of Pediatric Laboratory, Affiliated Children's Hospital of Jiangnan University, Wuxi Children's Hospital, 214023, Wuxi, Jiangsu, China

^c Department of Pediatric Surgery, Affiliated Children's Hospital of Jiangnan University, Wuxi Children's Hospital, 214023, Wuxi, Jiangsu, China

^d State Key Laboratory of Reproductive Medicine, Research Institute for Reproductive Health and Genetic Diseases, Wuxi Maternity and Child Health Care Hospital, Affiliated Women's Hospital of Jiangnan University, 214002, Wuxi, Jiangsu, China

^e Guangzhou Women and Children's Medical Center, Guangzhou Medical University, Guangzhou, China

^f Key Laboratory of Birth Defects, Children's Hospital, Institutes of Biomedical Sciences, Fudan University, Shanghai, China

ARTICLE INFO

Keywords:

Necrotizing enterocolitis
Intestinal stem cells
Extracellular vesicles
Intestinal injury

ABSTRACT

The therapeutic potential of intestinal stem cell-derived extracellular vesicles (ISCs-EVs) in necrotizing enterocolitis (NEC) remains largely unexplored. This research aims to investigate the therapeutic effects of ISCs-EVs on NEC. Lgr5-positive ISCs were screened from the small intestine of mice by flow cytometry, and ISCs-EVs were isolated by density gradient centrifugation. Subsequently, ISCs-EVs were identified through transmission electron microscopy, nanoparticle tracking analysis, and western blotting. Subsequently, we evaluated the efficacy of ISCs-EVs in a mouse model of NEC and found that they enhanced survival (more than 20%), reduced intestinal damage (restore the number of intestinal crypts and decrease the expression of MPO and cleaved-caspase 3 in intestinal tissues), promoted angiogenesis (the mRNA expression of VEGF was increased by approximately 35%), and mitigated inflammation (decreased the level of MUC1, p-NF- κ B, IL-6 and TNF- α). Furthermore, in vitro assessments demonstrated that ISCs-EVs reduced apoptosis ($P < 0.01$) and stimulated proliferation ($P < 0.05$) of IEC-6 cells, while enhancing mucin secretion in LS174T cells. In summary, our study provides a comprehensive assessment of the therapeutic effects of ISCs-EVs on NEC, using both animal and cell models. This highlights their potential for use in NEC treatment.

1. Introduction

Necrotizing enterocolitis (NEC) is a critical gastrointestinal disorder that occurs in neonates, particularly premature infants, and is characterized by intestinal mucosal edema, bleeding, necrosis, and inflammatory cell infiltration [1]. This condition presents with insidious onset, rapid progression, and substantial risk, with severe cases leading to intestinal perforation, sepsis, shock, multi-organ failure, and even jeopardization of the life of the affected infants [2].

Although considerable progress has been made in the use of stem cell therapy to treat NEC, most advancements have been limited to

experimental NEC models [3]. To date, only one clinical study involving the use of bone marrow-derived stem cells (BMSCs) for NEC treatment has been reported [4]. The limited clinical applications of stem cell therapy can be attributed to several challenges.

First, the isolation and cultivation of stem cells poses inherent difficulties and may raise ethical concerns. Second, stem cell transplantation can trigger immune reactions and increase oncogenic risks [5, 6].

Stem cells exert their therapeutic effects primarily through paracrine signaling in NEC [7]. Recent studies have indicated that the efficacy of stem cell-derived extracellular vesicles (EVs) in NEC treatment is

* Corresponding author. Guangzhou Women and Children's Medical Center, Guangzhou Medical University, Guangzhou, China.

** Corresponding author. Affiliated Children's Hospital of Jiangnan University, Wuxi Children's Hospital, Wuxi, China.

*** Corresponding author. Affiliated Children's Hospital of Jiangnan University, Wuxi Children's Hospital, Wuxi, China.

E-mail addresses: qvip123@126.com (W. Jin), yuanfuqiang97@126.com (F. Yuan), zhouwenhao@fudan.edu.cn (W. Zhou).

¹ These authors contributed equally to this work.

comparable to that of direct stem cell application [8]. Unlike stem cell transplantation, EV therapy offers several advantages, including safety, convenience, and efficiency for NEC [9]. Consequently, stem cell-derived EVs are promising candidates for NEC treatment, potentially overcoming the limitations of direct stem cell transplantation.

In this study, we intended to explore the potential of intestinal stem cell-derived extracellular vesicles (ISCs-EVs) in alleviating NEC. To achieve this, we initially constructed a NEC mouse model and evaluated the influences of ISCs-EVs on intestinal injury, angiogenesis, and inflammation. Subsequently, we established an intestinal epithelial injury cell model and assessed the effects of ISCs-EVs on the functional phenotypes of IEC-6 cells. Furthermore, we investigated the impacts of ISCs-EVs on goblet cells both *in vivo* and *in vitro*. This research comprehensively evaluated the benefits of ISCs-EVs in the treatment of NEC and emphasized their potential for treating this disorder.

2. Methods

2.1. Isolation and identification of ISCs

Six to eight-week-old C57BL/6 J mice were obtained from Shanghai Jihui Experimental Animal Co., Ltd. The animal experimental protocol was approved by the Experimental Animal Ethics Committee of Fudan University. Mouse ISCs were isolated using established methods [10,11]. The mice were euthanized and 15 cm of the proximal small intestine was excised and washed with cold PBS. The intestine was then minced and incubated in 30 mM cold ethylene diamine tetraacetic acid (EDTA)-PBS buffer (Regal, China) on a shaker at 4 °C for 30 min. The tissue was transferred to a new tube, vigorously vortexed for 5 min with cold EDTA-PBS for 30 min, and allowed to stand for 30 s before the supernatant containing the crypt cells was carefully aspirated. This supernatant was re-added to the tube with cold EDTA-PBS and vortexed at 4 °C for another 30 min to fully release villi and crypts. Once settled, the crypt cell suspension was filtered through a 70- μ m cell sieve (Corning, USA) into a tube pre-coated with 1 % bovine serum albumin (BSA) and washed with cold PBS twice. Subsequently, the crypt cells were suspended in TrypLE Express solution (Thermo Fisher Scientific, USA) and incubated at 37 °C for 10 min. Subsequently, 10 % fetal bovine serum (FBS) was added to the cell suspension and filtered through a 40- μ m cell sieve (Corning). After washing twice with basal medium (Gibco, USA), the cells were stained with CD326 (EpcAM)/Lgr5, washed twice with PBS, and resuspended in the basal medium. Lgr5-labeled ISC were isolated from the CD326 cell population using flow cytometry (BD Biosciences).

The isolated ISCs were cultured in Advanced Dulbecco's Modified Eagle Medium/Nutrient Mixture F-12 (DMEM/F12) medium (Life Technologies, USA), which was replaced with serum-free medium when the confluence reached 50–70 % to prevent contamination by numerous bovine exosomes in FBS. The cells were further cultured for 48 h before collecting the supernatant for exosome extraction.

2.2. Extraction and validation of exosomes

The supernatant was subjected to differential centrifugation to obtain relatively pure EVs. They were added to a density gradient sucrose solution. After centrifugation, the layer enriched with EVs was collected. After another round of centrifugation, the precipitate was resuspended. Part of it was used for identification, and the remaining part was frozen and preserved at –20 °C.

Transmission electron microscopy (TEM), nanoparticle tracking analysis (NTA), and western blotting were performed to identify the EVs. EVs were fixed with paraformaldehyde (Macklin, China), and their morphology was observed using TEM (JEOL JEM-2100, Japan). The size distribution of the EVs was monitored using a laser particle size analyzer (Malvern Mastersizer 3000, UK). Western blotting was conducted to detect the EV markers, CD63 and Alix. Isometric Radio

Immunoprecipitation Assay (RIPA) lysis buffer (MedChemExpress, USA) was mixed with the extracted EVs, and the protein concentration was quantified using the Bicinchoninic Acid Assay (BCA) method. Equal amounts of protein samples were denatured for electrophoresis and transferred onto a polyvinylidene fluoride (PVDF) film (Millipore, USA). The film was then blocked with 5 % skim milk for 1 h and incubated with diluted primary antibodies, including anti-CD63 (bsm-60749R, 1:1000, Bioss), anti-Alix (ab88388, 1:2000, Abcam), and anti-GAPDH (92310, 1:1000, Cell Signaling Technology), overnight at 4 °C. After the film was rinsed with PBST, it was then reacted with diluted secondary antibody solution (ab97051, 1:10000, Abcam) at 25 °C for 1 h, followed by imaging using chemiluminescence reagents (Thermo Fisher Scientific).

2.3. Construction and treatment of NEC neonatal mouse model

Seventy 6-day-old C57BL/6 neonatal mice were randomly divided into four groups: model (n = 25), PBS (n = 23), ISCs-Exo (n = 15), and control (n = 7). An NEC mouse model was established using a combination of hypoxia, cold exposure, and artificial overfeeding. Specifically, neonatal mice in the model, PBS, and ISCs-EVs groups were administered a high-osmolarity mouse formula (15 g Similac (Abbott, USA) mixed with 75 mL Esbilac (Pet-Ag, USA)) via gavage (five times/day). After feeding, they were placed into a hypoxia chamber (ProOx-810, Tow-int, China) for 10 min (The hypoxia conditions were set as 5 % O₂ + 95 % N₂), accompanied with a 10 min cold stimulus at 4 °C. Hypoxic and cold stimuli were repeated twice daily, and the modeling lasted for four days. Mice in the PBS and ISCs-EVs groups were treated via intraperitoneal injection with 100- μ L PBS or ISCs-EVs (approximately 10¹¹ particles) everyday during the modeling [12–15]. The Control group received no treatment and were breast-fed by their mothers. All neonatal mice in the groups were fasted for 12 h after the final feeding, and intestinal tissues were collected after euthanasia. All animal experiments adhered to the Guide for the Care and Use of Laboratory Animals published by the National Institutes of Health (NIH Publications No. 85-23, revised 1996) and were approved by the Medical Ethics Committee for the Ethics of Animal Experiments at Jiangnan University.

2.4. Hematoxylin and eosin (H&E) staining

Fixed ileal tissues were cut into paraffin sections and H&E staining was performed. Mouse ileal tissue sections were successively dewaxed and rehydrated. The sections were then stained with hematoxylin (Beyotime, China) for 3 min and eosin (Beyotime) for 30 s. After staining, sections were dehydrated in an ethanol gradient, vitrified with xylene, and sealed with neutral gum. Intestinal morphological changes were independently observed by two pathologists under a light microscope and intestinal tissue injury was simultaneously scored.

2.5. Immunofluorescence staining

The paraffin sections were dewaxed, and antigen repair was conducted in EDTA buffer (pH 8.0) (Solarbio, China) using a microwave oven, and then blocked with 3 % BSA (Sigma-Aldrich, USA) for 30 min. Later, the appropriate primary antibody solutions were added to the slices, including anti-MPO (bs-41105R, 1:500), anti-cleaved caspase3 (bsm-33199M, 1:200), anti-cleaved Caspase3 (BSM-33199m, 1:200), anti-MUC2 (bs-60331R, 1:50), and hatched with the sections at 4 °C overnight. The following day, the sections were incubated with fluorescent secondary antibodies for 1 h in the dark, followed by nuclear staining with DAPI staining solution (Acme, China). All the antibodies used in this study were purchased from Bioss Biotechnology Co., Ltd. (China). Finally, the sections were observed under a fluorescence microscope.

2.6. Real-time quantitative polymerase chain reaction (RT-qPCR)

Initially, a mouse intestinal tissue homogenate was prepared and total RNA was extracted. The RNA was then inverse-transcribed into cDNA using the PrimeScript™ RT reagent Kit (Takara, Japan). Subsequently, the RT-qPCR reaction system was formulated by mixing cDNA, specific primers of *Vegf*, *Il-6*, *Tnf-α*, and TB Green® Premix Ex Taq™ II FAST qPCR (Takara). Amplification was performed using a qPCR instrument (Bio-Rad CFX96, USA). *GAPDH* was used as an internal reference gene in order to normalize the expression of other target genes. The sequences of primers were as follows: *Vegf*, forward: 5'-ACGGATCAAGCCTTGCAGC-3', reverse: 5'-CGCGAATTGACAGCAGCTCTG-3'; *Gapdh*, forward: 5'-GACTGTACAGATAACGACTTG-3', reverse: 5'-AACGTAGCTCAGATTCGACCA-3'; *Il-6*, forward: 5'-CTGGGAAATCGTGAAATGAG-3', reverse: 5'-GACTCTGGCTTGTCTTCTTGTTA-3'; *Tnf-α*, forward: 5'-GACCCCTTACTCTGACCC-3', reverse: 5'-AGGCTCCAGTGAATTCGGAA-3'.

2.7. Immunohistochemical staining

The paraffin sections were dewaxed and rehydrated, followed by antigen retrieval. Endogenous peroxidase activity was blocked with a hydrogen peroxide inhibitor for 10 min. The sections were then sequentially incubated with diluted primary and secondary antibodies. The information of antibodies was as follows: anti-MUC1 (ab109185, 1:250, Abcam), anti-p-NFκB (ab86299, 1:500, Abcam), anti-MUC2 (sc-59859, 1:100, SANTA CRUZ), and anti-PCNA (Cat#307901, 1:100, Biologend), goat anti-rabbit IgG (ab205718, 1:5000, Abcam), and goat anti-mouse IgG (ab205719, 1:5000, Abcam). After washing, the diaminobenzidine (DAB) chromogenic agent (Biodragon, China) was applied, and the sections were incubated for 8 min, followed by thorough rinsing. Finally, the sections were counterstained with hematoxylin for 1 min, dehydrated, until transparent, and sealed.

2.8. Enzyme-linked immunosorbent assay (ELISA)

The levels of IL-6, TNF-α, and IL-18 in mouse serum and cultured intestinal epithelial cell culture supernatant were detected following the instructions of ELISA kit. All the ELISA kits were purchased from Beyotime Biotechnology. Standards were gradient diluted, and 100 μL of the diluted standards and samples were added into a 96-well plate. After introducing the enzyme-labeled antibody, the plate was placed in 37 °C incubator for 1 h. After multiple washes with washing buffer, a chromogenic reagent was added. Following incubation for 10 min, stop solution was added. Subsequently, the OD450 was measured using a microplate reader (Tecan Infinite 200Pro, Switzerland). A standard curve was drawn and the concentrations of inflammatory factors in each sample were calculated.

2.9. Counting of bacteria in mouse colon tissue

Colon tissues from each group of mice were homogenized, and the homogenate was centrifuged at 12000×g for 10 min at 4 °C to collect the supernatant. Subsequently, the supernatant was evenly spread on blood agar plates and cultured in an incubator at 37 °C. The bacterial colony counts on the culture plates were determined after 48 h.

2.10. PeriodicAcid-schiff (PAS) staining

Staining was performed according to the instructions provided with the PAS Staining Kit (Solarbio). The paraffin sections of the terminal ileum were dewaxed, rehydrated, and treated with an oxidizing agent for 7 min. After rinsing, the Schiff reagent was applied for 15 min and stained with hematoxylin for 2 min. The sections were differentiated in an acidic differentiation solution for 5 s and rinsed with running water for 10 min. Subsequently, a series of steps, including dehydration until

transparent and sealing were performed, and the sections were observed under a microscope.

2.11. Cell culture and treatment

LS174T cells were obtained from Procell (China) and IEC-6 cells were purchased from iCell Bioscience (China). All cells were cultured in their respective specialized media. ISCs-EVs (approximately 10⁶ particles/cell) [14,16,17] were added to the culture medium of LS174T cells to investigate their impact on goblet cells. IEC-6 cells were exposed to 18 μg/mL of Lipopolysaccharide (LPS) for 48 h to induce epithelial injury.

2.12. Western blotting of goblet cell markers

MUC2 expression was evaluated using western blotting. The primary antibody used was an anti-MUC2 antibody (ab133555, 1:3000, Abcam). The experimental procedure was the same as that used for EV marker detection.

2.13. Terminal-deoxynucleotidyl Transferase Mediated Nick End labeling (TUNEL) staining

An in-Situ Cell Death Detection Kit, Fluorescein (Roche, Switzerland), was used to assess apoptosis in mouse IECs. The dewaxed and rehydrated paraffin sections were treated with Proteinase K at 37 °C for 20 min. The sections were then treated with cell permeabilization solution for 10 min. After rinsing with PBS, the TUNEL reaction mixture was added, and the sections were placed in a wet box at 37 °C for 1 h. The nuclei were then stained with dihydrochloride (DAPI). The sections were sealed, observed, and imaged using a fluorescence microscope.

2.14. Flow cytometry

Apoptosis was assessed using flow cytometry. IEC-6 cells were seeded in six-well plates and cultured for at least 16 h. After treatment, cells were collected and the concentration was adjusted to 1 × 10⁶/mL, and then stained with 5 μL of Annexin V-FITC and PI (Thermo Fisher Scientific). Apoptosis was measured using a flow cytometer (BD FACSAria III, USA).

2.15. 5-Ethynyl-2'-deoxyuridine (EdU) staining

The propagation of IEC-6 cells was evaluated using an EdU Cell Proliferation Assay Kit (Solarbio). Briefly, cells in 96-well plates were treated accordingly. Then the prepared 50 μM EdU medium was added (100 μL/well), incubated for 2 h and rinsed with PBS. After 30 min incubation with cell fixation at room temperature, 50 μL of glycine solution was introduced into each well. Following PBS rinsing, 100 μL of TritonX-100 and Apollo solution was added and left at 25 °C for 30 min away from light. After rinsing, the cell nuclei were stained with Hoechst 33342 and an immediate microscopic examination was performed.

2.16. Scratch test

This assay was used to assess the healing ability of IEC-6 cells. On the first day, 5 × 10⁵ cells/well were seeded into each well. On the following day, a straight line was drawn across the confluent cell layer using a sterile pipette tip. After washing away the detached cells, the medium was replaced with a serum-free culture medium. After 24 h of incubation, the healing of the scratch was observed and recorded under a microscope.

2.17. Transwell assay

One day prior to the experiment, Matrigel (Corning) was diluted and evenly coated on the upper transwell chamber (Corning). After allowing

it to solidify, serum-free medium was added for hydration. On the second day, IEC-6 cells that reached approximately 80 % confluence, were spread into the upper chamber with a density of $2.5 \times 10^5/\text{mL}$, and 500 μL of complete medium was added in the lower chamber. After 24–48 h of culture, the Transwell chamber was removed, and the Matrigel and cells in the upper chamber were gently wiped off using a cotton swab and fixed in a fixative for 20 min. The cells were then stained with a 0.1 % crystal violet solution (Nanjing Reagent, China). After another round of washing, cells were dried and examined under a microscope.

2.18. Statistical analysis

GraphPad Prism 9 software was applied for the statistical analysis. Data were presented as the mean \pm standard deviation. Student's t-test or one-way analysis of variance was used for data comparisons between two or more groups. Survival rates were analyzed using the log-rank test. $P < 0.05$ was considered statistically significant.

3. Results

3.1. Identification of ISCs-EVs

Initially, IECs were split following a previously described method [10,11,18], and Lgr5-positive ISCs were isolated from the small intestines of the mice using flow cytometry (Fig. S1). Subsequently, the EVs secreted by ISCs were isolated and characterized. TEM revealed that EVs derived from mouse ISCs exhibited typical bilayer membrane vesicular structures, with diameters ranging from approximately 30–100 nm (Fig. 1A). Data of NTA indicated that the particle size range of the obtained EVs was 95.4 ± 18.9 nm, with an average size of 87 nm (Fig. 1B). Furthermore, western blotting validated the positive expression of Alix and CD63 on the surface of the extracted EVs (Fig. 1C). These results validate successful isolation of EVs derived from mouse ISCs.

3.2. ISCs-EVs alleviate intestinal damage in NEC mice

To investigate the function of ISC-Exos in NEC, we established an NEC mouse model induced by high-osmolarity feeding, hypoxia, and cold stimulation, and treated the mice with ISC-Exos. Survival rates in the model and PBS groups significantly decreased within 10 days of treatment, whereas they markedly increased after treatment with ISCs-EVs (Fig. 2A). The expression of the pro-angiogenic gene *Vegf* was low in the model and PBS groups, whereas ISCs-EVs treatment significantly elevated the levels of *Vegf* ($P < 0.01$, Fig. 2B). H&E staining demonstrated that treatment ameliorated intestinal damage induced by NEC, leading to a reduction in histological scores ($P < 0.05$, Fig. 2C). Furthermore, the immunofluorescence staining results indicated that the number of MPO-positive (green) and cleaved caspase-3-positive (red) cells in the terminal ileum dramatically increased in the model and PBS groups, and the number of MPO-positive ($P < 0.01$) and cleaved caspase-3-positive ($P < 0.05$) cells markedly decreased after treatment

with ISCs-EVs (Fig. 2D). These findings suggest that ISCs-EVs enhance the survival of NEC mice, reduce intestinal damage, improve neutrophil infiltration and apoptosis, and promote intestinal angiogenesis.

3.3. ISCs-EVs ameliorate intestinal inflammation in NEC mice

Intestinal inflammation is a hallmark of NEC. Therefore, we investigated whether ISCs-EVs can improve intestinal inflammation in mice with NEC. Immunohistochemical staining results showed decreased expression of MUC1 and increased p-NF- κ B in the colon tissues of NEC mice, which were reversible with ISCs-EVs treatment (Fig. 3A). Furthermore, we confirmed that ISCs-EVs lowered the levels of inflammatory cytokines IL-6 and TNF- α in the serum (Fig. 3B) and colon (Fig. 3C) of NEC mice ($P < 0.01$). Bacterial counts in mouse colonic tissues also confirmed that ISCs-EVs inhibited bacterial invasion of NEC mouse colonic tissues ($P < 0.01$, Fig. 3D). These results suggested that ISCs-EVs effectively ameliorated intestinal inflammation in NEC mice.

3.4. ISCs-EVs promote goblet mucin secretion in vivo

Goblet cells play a crucial role in maintaining the integrity and stability of the intestinal mucosa by secreting protective mucous barriers, including mucin, which forms a protective layer on the intestinal surface. Therefore, we used immunofluorescence assays to detect mucin protein expression levels in goblet cells. A significant increase in the mucin protein expression was observed in the group treated with ISCs-EVs (Fig. 4A). These findings suggested that ISCs-EVs promoted mucin secretion by goblet cells in vivo.

3.5. ISCs-EVs reduce apoptosis of IECs and promote their proliferation in vivo

IECs, which serve as the first line of defense against pathogenic microorganisms in the intestine, are essential components of the intestinal mucosal barrier. Therefore, we investigated the protective effects of ISCs-EVs against IECs. Significant apoptosis was observed in the IECs of NEC mice, which was markedly reduced after treatment with ISCs-EVs (Fig. 5A). Furthermore, the expression level of PCNA, which reflects the cell proliferation status, was decreased in the small intestinal tissues of mice in the model group and partially restored after treatment with ISCs-EVs (Fig. 5B). These findings suggest that ISCs-EVs reduce IEC apoptosis and promote IEC proliferation in vivo.

3.6. ISCs-EVs promote mucin secretion of goblet cells in vitro

Furthermore, we investigated whether ISCs-EVs could promote mucin production in goblet cells in vitro using LS174T cells. Results of PAS staining and western blotting confirmed that ISCs-EVs promoted mucin production in LS174T cells ($P < 0.01$, Fig. 6A and B). These results indicate that ISCs-EVs can promote goblet cell mucin secretion in vitro.

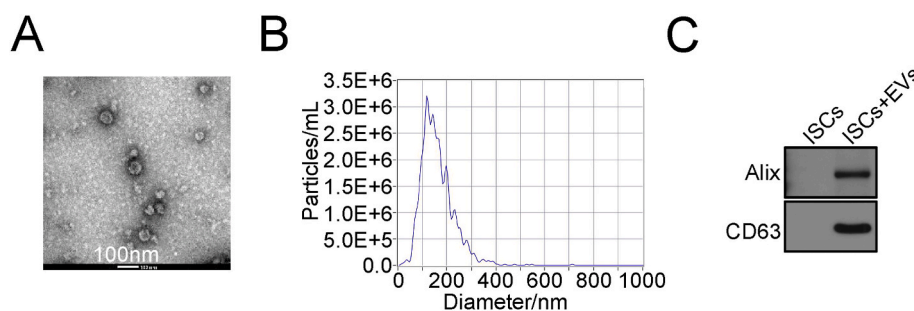


Fig. 1. Identification of ISCs-EVs. A. TEM images of the isolated ISCs-EVs. B. The particle size range of ISCs-EVs. C. Western blot analysis of EVs markers Alix and CD63.

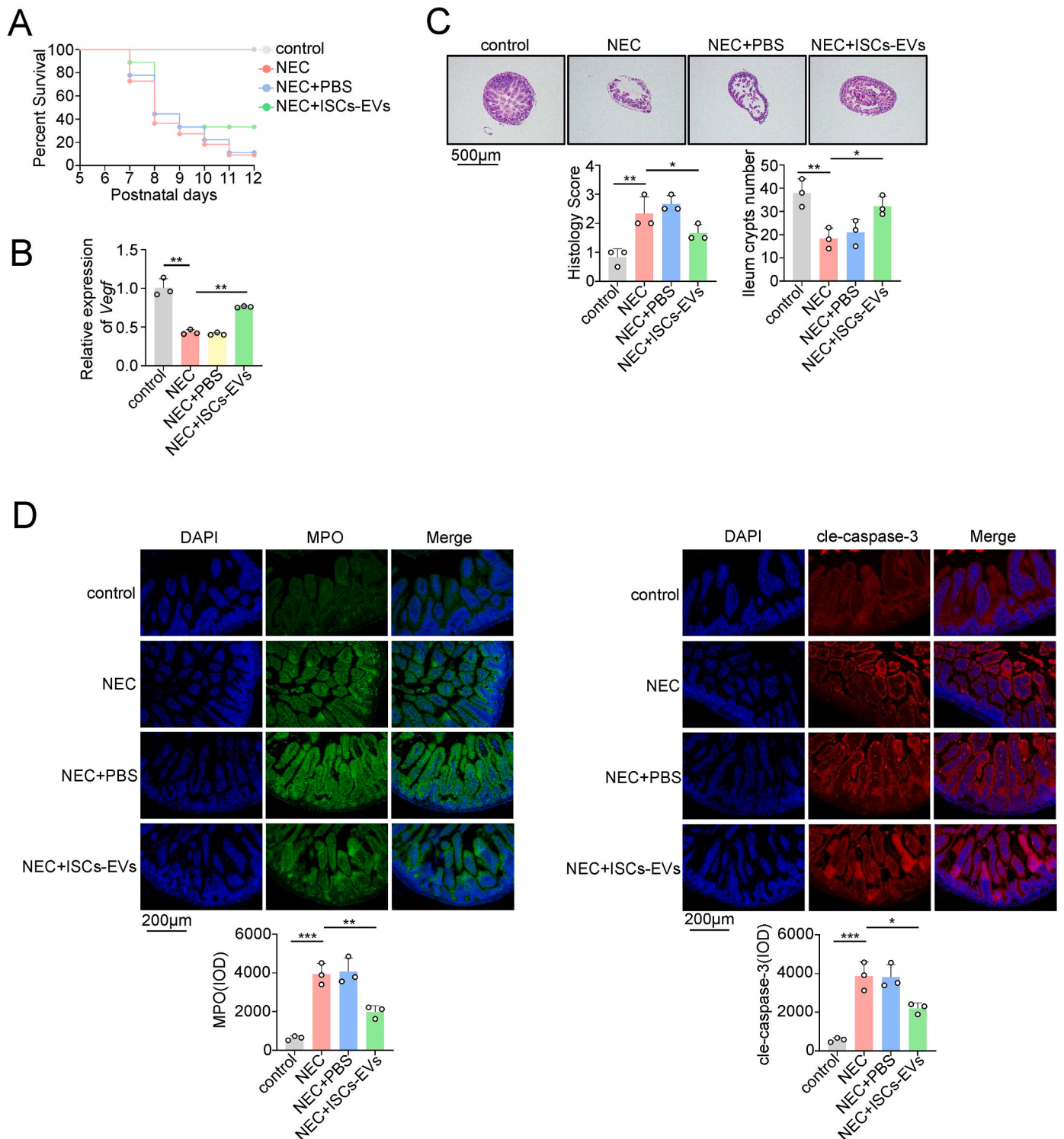


Fig. 2. ISCs-EVs enhance survival and alleviate intestinal damage in NEC mice. **A.** Survival rate of mice in control, model, PBS and ISCs-EVs groups. **B.** Relative mRNA expression level of *Vegf* in the four groups. **C.** H&E staining of the terminal ileum and the histology scores of each group. **D.** Immunofluorescence staining of MPO and Cleaved-caspase-3 in terminal ileum. * $p < 0.05$, ** $p < 0.01$, *** $p < 0.001$.

3.7. ISCs-EVs reduce apoptosis and promote proliferation of IECs in vitro

We explored the in vitro effects of ISCs-EVs on IECs. Lipopolysaccharide-induced IEC-6 cells were used as an in vitro model of intestinal epithelial cell damage. Consistent with our in vivo findings, ISCs-EVs inhibited the apoptosis of IEC-6 cells (Fig. 7A). Moreover, the number of EdU-positive cells in the model group decreased, whereas

treatment with ISCs-EVs resulted in a marked increase in EdU-positive IEC-6 cells ($P < 0.05$, Fig. 7B). These results indicated that ISCs-EVscan reduce apoptosis and promote IEC proliferation in vitro.

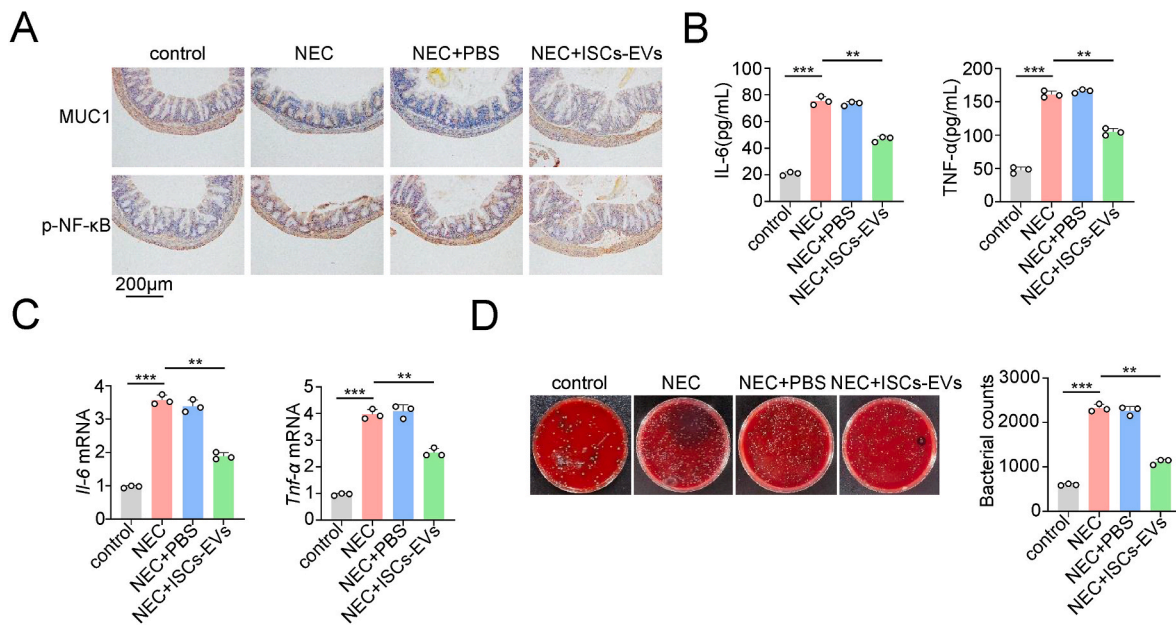


Fig. 3. ISCs-EVs ameliorate intestinal inflammation in NEC mice. A. Immunohistochemical staining of MUC1 and p-NF- κ B in the colonic tissues of NEC mice in control, model, PBS and ISCs-EVs groups. The contents of inflammatory cytokines IL-6 and TNF- α in the serum were detected by ELISA assay (B) and colon of NEC mice (C) were detected by RT-qPCR. D. The bacterial counts in mouse colonic tissues. * $p < 0.05$, ** $p < 0.01$, *** $p < 0.001$.

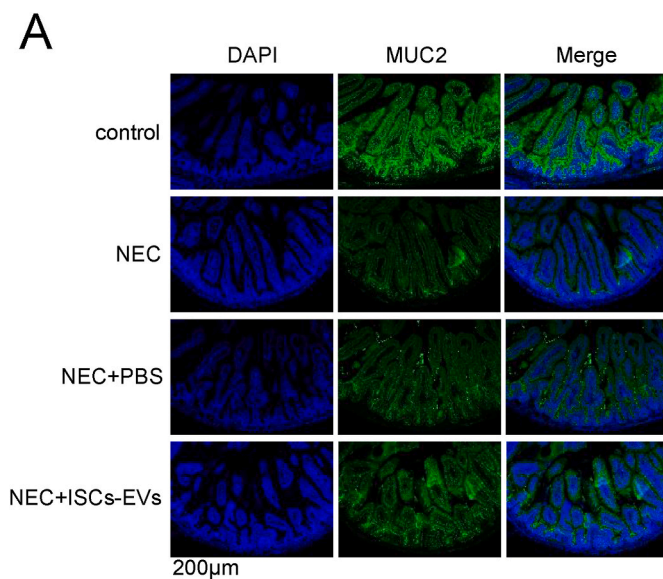


Fig. 4. ISCs-EVs promote goblet cell mucin secretion in vivo. A. Immunofluorescence staining of MUC2 in mice terminal ileum.

3.8. ISCs-EVs suppress inflammatory responses and restore intestinal epithelial repair capability in vitro

We investigated whether ISCs-EVs could suppress inflammatory responses and promote repair of the intestinal epithelium in vitro. ELISA was performed to assess the expression levels of inflammatory cytokines in the supernatant of damaged IECs. The secretion of both IL-6 and IL-18 was notably downregulated in IEC-6 cells after treatment with ISCs-EVs ($P < 0.05$, Fig. 8A). Additionally, ISCs-EVs enhanced the migration ($P < 0.05$, Fig. 8B) and invasion ($P < 0.01$, Fig. 8C) of IECs. These results confirmed that ISCs-EVs suppress inflammatory responses and restore the repair capability of the intestinal epithelium in vitro.

4. Discussion

Research on the use of stem cells or stem cell-derived exosomes for NEC treatment has steadily increased. However, most studies have focused on BMSCs, amniotic fluid, umbilical cords, and neural stem cells [19]. McCulloh et al. conducted a comparative analysis of the therapeutic effects of MSCs and neural stem cells derived from the amniotic fluid, BMSCs, and neonatal intestinal neural stem cells in an NEC rat model [20]. Their findings indicated that all four stem cell types demonstrated nearly equivalent efficacy in suppressing NEC occurrence and reducing its severity.

Given the ethical and safety concerns associated with the direct use of stem cells for NEC treatment, McCulloh et al. explored the therapeutic potential of exosomes derived from stem cells in rat NEC pups [21]. They discovered that stem cell exosomes were as effective as their parent stem cells in reducing the incidence and severity of NEC. This suggests that stem cell-derived exosomes may serve as promising candidates for cell-free therapeutic approaches for NEC. In this study, we used EVs derived from ISCs to treat experimental NEC, which yielded promising results. ISCs are widely recognized for their role in maintaining intestinal homeostasis [22]. However, compared with other commonly used stem cells for NEC treatment, isolating and purifying ISCs is more complex, which could limit their application. We used flow cytometry to select CD326- and Lgr5-positive ISCs from mouse intestinal crypts and villi. Subsequently, we isolated EVs from ISCs through ultracentrifugation and validated them by TEM, NTA, and Western blot analyses.

NEC is associated with immune system imbalance, and exacerbated inflammatory injury is linked to increased levels of proinflammatory mediators. These mediators can compromise the tight junction barrier of the intestinal epithelium, leading to increased intestinal permeability, bleeding, necrosis, and perforation of the intestinal mucosa [23]. Our results show that ISCs-EVs reduced neutrophil infiltration in the terminal ileum of NEC mice, decreased levels of proinflammatory cytokines, IL-6 and TNF- α , in the serum and colon, and reduced bacterial counts in colon tissues of NEC mice. MUC1 is a transmembrane glycoprotein that plays crucial roles in infection and inflammation. It exerts anti-inflammatory effects by interfering with the NF- κ B signaling pathway [24]. Following treatment with ISCs-EVs, we observed an increase in MUC1 expression and a decrease in p-NF- κ B levels in the colon

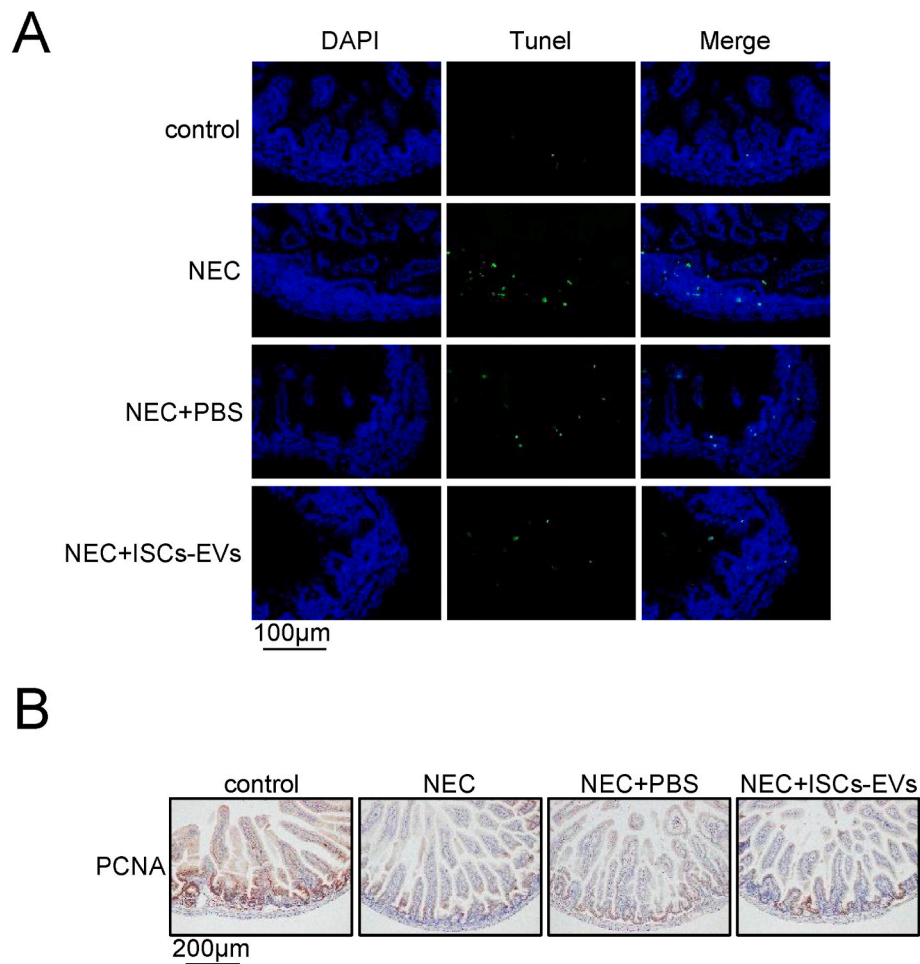


Fig. 5. ISCs-EVs reduce IEC apoptosis and promote their proliferation in vivo. A. TUNEL staining of IECs of mice in control, model, PBS and ISCs-EVs groups. B. Immunohistochemical staining of PCNA in the small intestinal tissues of mice.

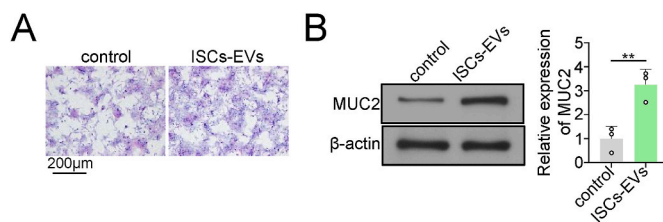


Fig. 6. ISCs-EVs promote mucin secretion of goblet cells in vitro. A. PAS staining of LS174T cells in the control and ISCs-EVs groups. B. Western blot analysis of MUC2 in LS174T cells. * $p < 0.05$, ** $p < 0.01$, *** $p < 0.001$.

tissues of NEC mice. These findings suggest that ISCs-EVs mitigate pathological intestinal damage in neonatal NEC mice by reducing intestinal inflammation.

As secretory cells in the intestinal epithelium, mucins and other components secreted by goblet cells constitute a protective mucus barrier covering the surface of the intestinal tract, which is an important component of the intestinal immune defense line [25]. Goblet cells are involved in the development of various intestinal diseases, including NEC [26]. In the in vivo study, we confirmed that ISCs-Exo promoted the quantity of goblet cells in the villi of the terminal ileum in NEC mice, along with an upregulation of MUC2 and GRP94. MUC2 is the major mucin secreted by goblet cells, and its upregulation indicates the restoration of intestinal epithelial barrier function [27]. GRP94 is one of the most abundant molecular chaperones in the endoplasmic reticulum

and is crucial for maintaining normal intestinal barrier function [28]. In this study, we used LS174T cells, a goblet cell-like colorectal cancer cell line, to probe the function of ISCs-Exo in the activity of goblet cell in vitro. Mucin is a glycoprotein secreted by goblet cells, contributing to intestinal protection [28]. PAS staining indicated that ISCs-Exo increased mucin production in LS174T cells. TFF3 and MUC2 are markers expressed by goblet cells, and ISCs-Exo promoted the expression of TFF3 and MUC2 in LS174T cells. Our research suggests that ISCs-Exo may enhance the recovery of intestinal barrier function in NEC neonatal mice by increasing the number and activity of goblet cells. This is in accordance with the findings of Li et al., who discovered that milk-derived exosomes could improve activity of goblet cells and prevent NEC development [29].

In addition to the abnormal secretion of goblet cells causing dysfunction in the intestinal barrier, excessive cell death of IECs is also an important factor contributing to NEC [30]. Here, we found that ISCs-Exo effectively suppressed apoptosis of IECs in NEC mice, as well as in LPS-induced IEC-6 and IEC-18 epithelial injury cell models, while promoting their proliferation. The healing and regenerative capacity of IECs are crucial for the repair of intestinal barrier damage. This research also highlighted the ability of ISCs-Exo to facilitate the functional recovery of IECs. Similarly, Rager et al. discovered that exosomes from BMSCs significantly enhanced the wound healing ability of IEC-6 cells, thereby protecting the intestine from NEC [31].

Overall, our study underscores the therapeutic potential of ISCs-EVs for treating NEC. Nevertheless, there is limited knowledge regarding the mechanisms by which ISCs-EVs exert their effects and bioactive

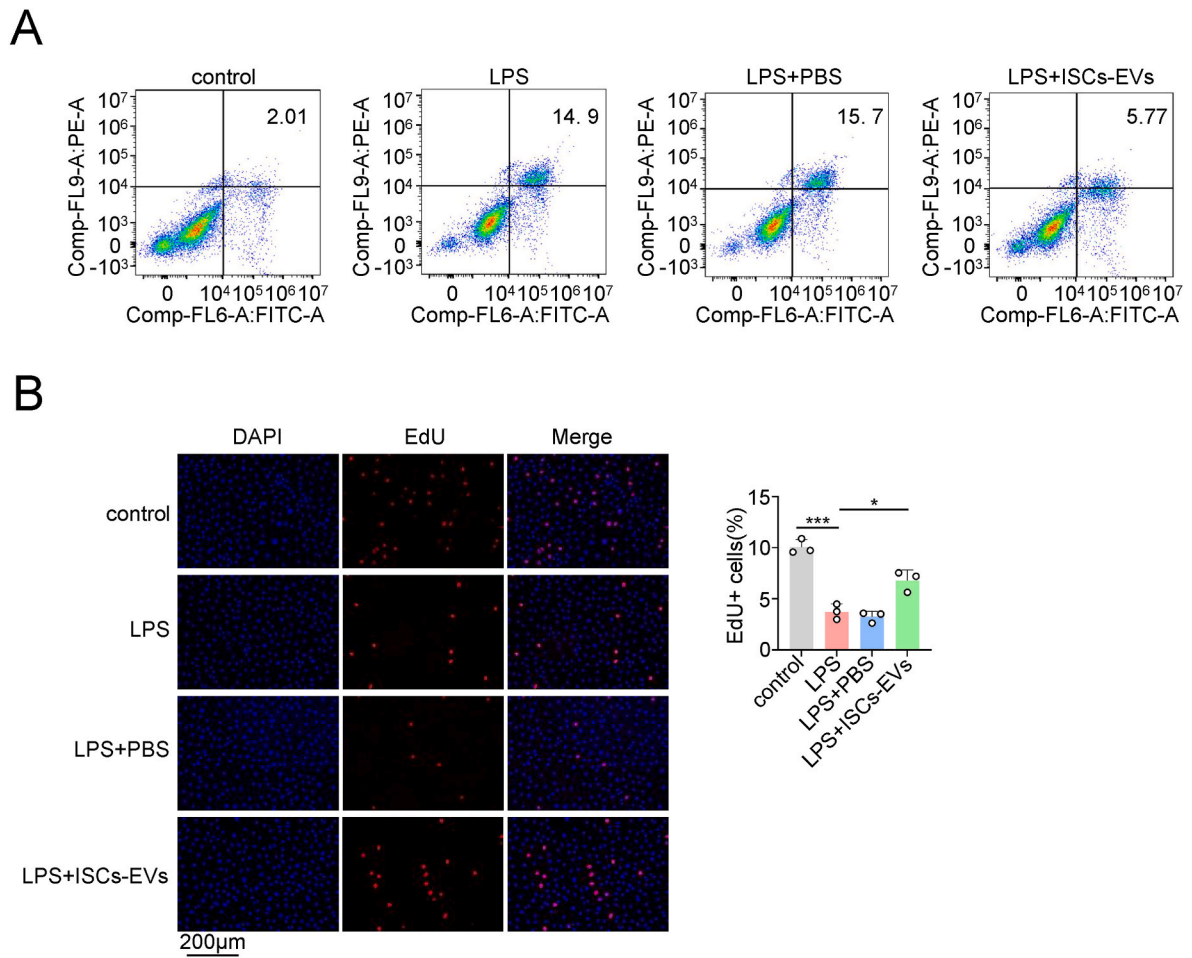


Fig. 7. ISCs-EVs reduce apoptosis and promote proliferation of IECs in vitro. **A.** Cell apoptosis of LPS-induced IEC-6 cells in control, model, PBS and ISCs-EVs groups was assessed by flow cytometry. **B.** EdU assay was performed to evaluate the proliferation of IEC-6 cells. * $p < 0.05$, ** $p < 0.01$, *** $p < 0.001$.

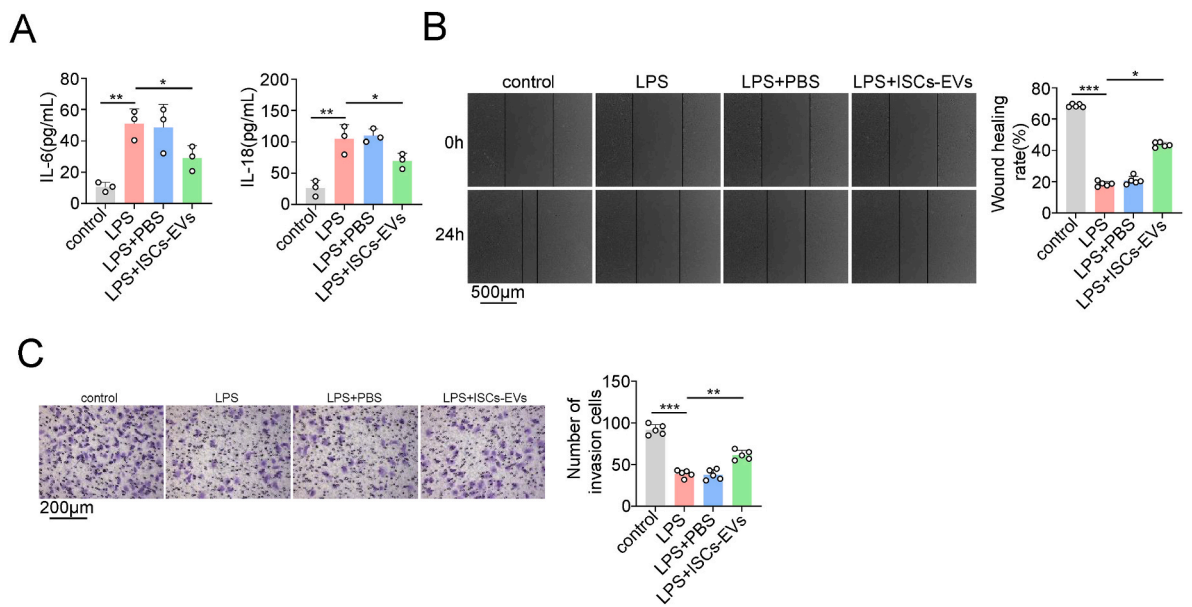


Fig. 8. ISCs-EVs suppress inflammatory responses and restore intestinal epithelial repair capability in vitro. **A.** The concentration of IL-6 and IL-18 in the supernatant of LPS-induced IEC-6 cells in control, model, PBS and ISCs-EVs groups was assessed by ELISA. Cell migration (**B**) and invasion (**C**) capacity was evaluated by scratch assay and Transwell assay, respectively. * $p < 0.05$, ** $p < 0.01$, *** $p < 0.001$.

mediators they contain. The preparation processes for ISCs and ISCs-EVs still lack unified standards, making it challenging to achieve large-scale commercial production. To date, there have been no clinical experiments on the use of ISCs or ISC-derived EVs for NEC, and the clinical indications, treatment timing, administration routes, and effective dosages for treatment using this approach remain undefined. Furthermore, although EVs are typically regarded as having lower immunogenicity than ISCs, the potential immunogenicity of ISCs-EVs is still a key concern in the imperfect development of the neonatal immune system. Hence, additional studies are necessary to explore the therapeutic mechanisms of ISCs-EVs in NEC and confirm their safety and efficacy in a clinical setting through long-term follow-up of NEC mouse models. We anticipate that our study will provide valuable insights for future clinical practice and treatment strategies.

CRediT authorship contribution statement

Le Zhang: Writing – original draft, Visualization, Methodology, Investigation, Formal analysis. **Jiahong Li:** Writing – original draft, Methodology, Investigation. **Qiwen Wan:** Writing – original draft, Methodology, Investigation. **Chaozhi Bu:** Methodology, Investigation. **Weilai Jin:** Writing – review & editing, Supervision, Data curation, Conceptualization. **Fuqiang Yuan:** Writing – review & editing, Supervision, Data curation, Conceptualization. **Wenhao Zhou:** Writing – review & editing, Supervision, Project administration, Funding acquisition, Data curation, Conceptualization.

Ethical approval

This study was approved by the Ethics Committee of Jiangnan University (JN.NO20201115c0701230[309]), and all methods were implemented in accordance with the guidelines and regulations of animal ethics standards.

Declaration of competing interest

The authors declare the following financial interests/personal relationships which may be considered as potential competing interests: Le Zhang reports financial support was provided by Wuxi Health Committee. Le Zhang reports financial support was provided by Wuxi City People's Government. If there are other authors, they declare that they have no known competing financial interests or personal relationships that could have appeared to influence the work reported in this paper.

Acknowledgments

This work was supported by the Top medical expert team of Wuxi Taihu Talent Plan (Grant Nos. DJTD202106 and GDTD202105); Medical Key Discipline Program of Wuxi Health Commission (Grant Nos. ZDXK2021007 and CXTD2021005); Top Talent Support Program for young and middle-aged people of Wuxi Health Committee (Grant No. BJ2023090); Scientific Research Program of Wuxi Health Commission (Grant No. Z202109, M202208); Jiangnan University Wuxi School of Medicine Subject Development Fund (Grant No. YXXK2024092610); and Wuxi Science and Technology Development Fund (Grant Nos. N20202003 and Y20222001).

Appendix A. Supplementary data

Supplementary data to this article can be found online at <https://doi.org/10.1016/j.mcp.2024.101997>.

Data availability

Data will be made available on request.

References

- [1] J.W. Duess, et al., Necrotizing enterocolitis, gut microbes, and sepsis, *Gut Microb.* 15 (1) (2023) 2221470.
- [2] M. Alganabi, et al., Recent advances in understanding necrotizing enterocolitis, *F1000Res* 8 (2019).
- [3] C. Pisano, G.E. Besner, Potential role of stem cells in disease prevention based on a murine model of experimental necrotizing enterocolitis, *J. Pediatr. Surg.* 54 (3) (2019) 413–416.
- [4] H. Akduman, et al., Successful mesenchymal stem cell application in supraventricular tachycardia-related necrotizing enterocolitis: a case report, *Fetal Pediatr. Pathol.* 40 (3) (2021) 250–255.
- [5] N.A. Drucker, et al., Stem cell therapy in necrotizing enterocolitis: current state and future directions, *Semin. Pediatr. Surg.* 27 (1) (2018) 57–64.
- [6] J.S. O'Connell, et al., Treatment of necrotizing enterocolitis by conditioned medium derived from human amniotic fluid stem cells, *PLoS One* 16 (12) (2021) e0260522.
- [7] F. Balsamo, et al., Amniotic fluid stem cells: a novel treatment for necrotizing enterocolitis, *Front Pediatr* 10 (2022) 1020986.
- [8] X. Hu, et al., Comparison and investigation of exosomes from human amniotic fluid stem cells and human breast milk in alleviating neonatal necrotizing enterocolitis, *Stem Cell Rev Rep* 19 (3) (2023) 754–766.
- [9] X. Yan, et al., LncRNA and mRNA profiles of human milk-derived exosomes and their possible roles in protecting against necrotizing enterocolitis, *Food Funct.* 13 (24) (2022) 12953–12965.
- [10] S.Y. Chen, J.F. Chen, FACS isolation of mouse intestinal stem cell, *Bio-101* 9 (22) (2019) e1010306.
- [11] K.P. O'Rourke, et al., Isolation, culture, and maintenance of mouse intestinal stem cells, *Bio Protoc* 6 (4) (2016).
- [12] A. Georgievski, et al., Acute lymphoblastic leukemia-derived extracellular vesicles affect quiescence of hematopoietic stem and progenitor cells, *Cell Death Dis.* 13 (4) (2022) 337.
- [13] A.F. Saleh, et al., Extracellular vesicles induce minimal hepatotoxicity and immunogenicity, *Nanoscale* 11 (14) (2019) 6990–7001.
- [14] L.T. Vu, et al., Tumor-secreted extracellular vesicles promote the activation of cancer-associated fibroblasts via the transfer of microRNA-125b, *J. Extracell. Vesicles* 8 (1) (2019) 1599680.
- [15] O.P. Wiklander, et al., Extracellular vesicle in vivo biodistribution is determined by cell source, route of administration and targeting, *J. Extracell. Vesicles* 4 (2015) 26316.
- [16] A. Longatti, et al., High affinity single-chain variable fragments are specific and versatile targeting motifs for extracellular vesicles, *Nanoscale* 10 (29) (2018) 14230–14244.
- [17] S.O. Piryan, et al., Endothelial cell-derived extracellular vesicles mitigate radiation-induced hematopoietic injury, *Int. J. Radiat. Oncol. Biol. Phys.* 104 (2) (2019) 291–301.
- [18] C.M. Nefzger, et al., A versatile strategy for isolating a highly enriched population of intestinal stem cells, *Stem Cell Rep.* 6 (3) (2016) 321–329.
- [19] R. Zeng, et al., Stem cells and exosomes: promising candidates for necrotizing enterocolitis therapy, *Stem Cell Res. Ther.* 12 (1) (2021) 323.
- [20] C.J. McCulloh, et al., Stem cells and necrotizing enterocolitis: a direct comparison of the efficacy of multiple types of stem cells, *J. Pediatr. Surg.* 52 (6) (2017) 999–1005.
- [21] C.J. McCulloh, et al., Treatment of experimental necrotizing enterocolitis with stem cell-derived exosomes, *J. Pediatr. Surg.* 53 (6) (2018) 1215–1220.
- [22] P.Y. Xing, S. Pettersson, P. Kundu, Microbial metabolites and intestinal stem cells tune intestinal homeostasis, *Proteomics* 20 (5–6) (2020) e1800419.
- [23] X. Cai, A. Golubkova, C.J. Hunter, Advances in our understanding of the molecular pathogenesis of necrotizing enterocolitis, *BMC Pediatr.* 22 (1) (2022) 225.
- [24] W. Li, et al., MUC1-C drives stemness in progression of colitis to colorectal cancer, *JCI Insight* 5 (12) (2020).
- [25] J.K. Gustafsson, M.E.V. Johansson, The role of goblet cells and mucus in intestinal homeostasis, *Nat. Rev. Gastroenterol. Hepatol.* 19 (12) (2022) 785–803.
- [26] S. Yang, M. Yu, Role of goblet cells in intestinal barrier and mucosal immunity, *J. Inflamm. Res.* 14 (2021) 3171–3183.
- [27] A. Tawiah, et al., High MUC2 mucin expression and misfolding induce cellular stress, reactive oxygen production, and apoptosis in goblet cells, *Am. J. Pathol.* 188 (6) (2018) 1354–1373.
- [28] B. Liu, et al., Essential roles of grp94 in gut homeostasis via chaperoning canonical Wnt pathway, *Proc Natl Acad Sci U S A* 110 (17) (2013) 6877–6882.
- [29] B. Li, et al., Bovine milk-derived exosomes enhance goblet cell activity and prevent the development of experimental necrotizing enterocolitis, *PLoS One* 14 (1) (2019) e0211431.
- [30] S. Yang, et al., Programmed death of intestinal epithelial cells in neonatal necrotizing enterocolitis: a mini-review, *Front Pediatr* 11 (2023) 1199878.
- [31] T.M. Rager, et al., Exosomes secreted from bone marrow-derived mesenchymal stem cells protect the intestines from experimental necrotizing enterocolitis, *J. Pediatr. Surg.* 51 (6) (2016) 942–947.